Analysis of autogram performance for rolling element bearing diagnosis by using different data sets

Analysis of Autogram performance for rolling element bearing diagnosis by using different data sets

Ali Moshrefzadeh, Alessandro Fasana, and Luigi Garibaldi

Politecnico di Torino, Corso Duca degli Abruzzi, 24
10129 Torino, Italy
ali.moshrefzadeh@polito.it

Abstract. Rolling element bearings are one of the most important component in every rotating machinery. As a result, their diagnosis before occurrence of any catastrophic failure is of vital importance and vibration based diagnosis is very popular approach. In this paper, the performance of a recently proposed method, Autogram, will be investigated on different data sets provided by Politecnico di Torino and University of Cincinnati. The results will be compared with other well-established methods such as Fast Kurtogram and Spectral Correlation

Keywords: Rolling element bearing, Diagnosis, Autogram, Fast Kurtogram, Fast Spectral Correlation, Experimental data

1 Introduction

Rolling element bearings are one of the key parts of every rotary machinery; therefore, their diagnosis is very important. Many researches have been done in this area but methods such as Fast Kurtogram [1] and Spectral Correlation (SC) [2] are among the mostly used approaches. In this paper, Autogram [3] is compared to theaforementioned methods and data from different test rigs are utilized to obtain a reliable assessment.

2 Theoretical background

2.1 Autogram

Autogram, as an effective method to find the suitable frequency band for demodulation, was introduced by Ref. [3] for diagnosis of rolling element bearings. This method takes advantage of cyclostationarity of the signals generated by bearing defects. Cyclostationary processes are non-stationary processes whose statistics are periodically varying.

The schematic of the method is in Figure 1. First, time signals are divided in frequency bands, according to a dyadic tree structure, by means of Maximal

Overlap (undecimated) Discrete Wavelet Packet Transform (MODWPT). Afterwards, AutoCorrelation (AC) of the squared envelope of the filtered signal is computed for each node as follows:

$$\hat{R}_{XX}(\tau) = \frac{1}{N-q} \sum_{i=1}^{N-q} X(t_i)X(t_i+\tau) \tag{1}$$

where X is the squared envelope of the filtered signal, N is the signal's length, $\tau = q/f_s$ is the delay factor, f_s is the sampling frequency and $q = 0, ..., N-1$. This step is beneficial as uncorrelated components, such as noise and random impulses, are removed while periodic impulses, related to bearings defects, are enhanced. Kurtosis, which indicates the impulsiveness of a signal, is then calculated with

$$\text{Kurtosis}(X) = \frac{\sum_{i=1}^{\frac{N}{2}} \left[\hat{R}_{XX}(i) - \min(\hat{R}_{XX}(\tau))\right]^4}{\left[\sum_{i=1}^{\frac{N}{2}} \left[\hat{R}_{XX}(i) - \min(\hat{R}_{XX}(\tau))\right]^2\right]^2}, \tag{2}$$

Kurtosis is consequently depicted as a colormap, named Autogram, as a function of decomposition level and frequency. Finally, the node with the highest kurtosis is selected and the Squared Envelope Spectrum (SES) is computed to investigate the presence of bearings characteristic frequencies. Examples of all the steps in the flowchart are given in Section 3.

Ref. [3] also proposed a modified version of Autogram, indicated as upper Autogram. In this case, the moving mean value of the AC is calculated by

$$\overline{X}_T(i) = \frac{1}{k} \sum_{j=i}^{i+k-1} \hat{R}_{XX}(j) \tag{3}$$

where k is length of the signal to be averaged, typically a very small fraction of N.

Then, the points of the AC signal lower than the mean value are replaced by the mean value itself and kurtosis is computed by

$$\text{Kurtosis}_u(X) = \frac{\sum_{i=1}^{\frac{N}{2}} |\hat{R}_{XX}(i) - \overline{X}_T(i)|_+^4}{\left[\sum_{i=1}^{\frac{N}{2}} |\hat{R}_{XX}(i) - \overline{X}_T(i)|_+^2\right]^2} \tag{4}$$

where operators $|\ |_+$ indicates that only positive values are accepted and negative values are set to zero.

In a real case, the impulse generated by a bearing defect might excite the structure in different frequency ranges and/or multiple defects with various resonance frequencies exist in a machinery. As a result, selecting only one node for further investigation might not provide a comprehensive diagnostic information. To overcome the aforementioned drawback, Ref. [3] also defined Combined Squared Envelope Spectrum (CSES) in which for each level of decomposition

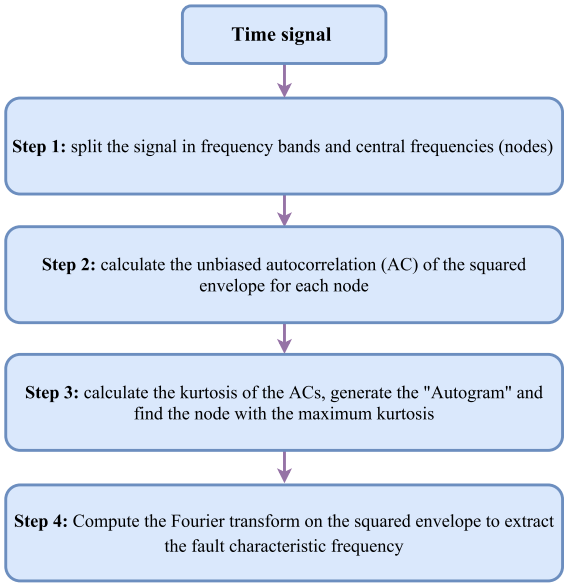

Fig. 1. Flowchart of the Autogram method [3]

the nodes with valuable information are chosen. Then, for each level normalized SESs (between 0 and 1) for all selected nodes are combined. The outcome is presented as a colormap with three variables: level of decomposition, frequency and summation of normalized SESs. Moreover, average CSES is defined as summation of CSES related to all levels. Examples are given in Section 3.

2.2 Spectral Correlation

Cyclic Spectral Analysis (CSA) [4] is a powerful approach for condition monitoring of rotary machinery which separates and describes different 2nd order cyclostationary components in terms of spectral frequency (f) and cyclic frequency (α). Spectral Correlation (SC) is one of the main tools for the CSA of machine signals and various methods have been proposed for its estimation. Among them, Averaged Cyclic Periodogram (ACP) or time-smoothed cyclic periodogram can be computed as follows [2]:

$$S_x^{ACP}(\alpha, f) = \frac{1}{K\|w\|^2 f_s} \sum_{i=1}^{K-1} X_w(i, f) X_w(i, f-\alpha)^* \tag{5}$$

$$\|w\|^2 = \sum_{n=0}^{L_w-1} |w_n|^2$$

where $*$ stands for complex conjugate, $X_w(f)$ is the short-time Fourier transform (SFTF) of the signal $x(t)$ with length N, w_n is the window function, $K = \frac{N-L_w}{R} + 1$ is the total number of averaged segments (total number of windows with length of L_w shifted by R samples). Recently Ref. [2] introduced a fast algorithm to compute the SC which substantially increases the computational efficiency. This approach will be used in this paper.

3 Results and discussion

In this section, first the performance of Autogram is compared with Fast Kurtogram by using a set of data acquired by the Center for Intelligent Maintenance Systems (IMS), University of Cincinnati [5,6]. Then, three data sets from the test rig assembled in the lab of the Dynamics and Identification Research Group in the Mechanical and Aerospace Engineering Department, Politecnico di Torino (DIRG-PoliTo), are studied. Two last cases are not diagnosable by using neither Kurtogram nor Autogram. The performance of CSES will then be shown and the results compared with the SC [2].

In the following plots, green dash-dot lines are depicted at the nominal shaft frequency, red dashed lines at harmonics of the expected fault frequency, and red dotted lines display the first order modulation sidebands around the fault frequency and its harmonics.

3.1 Test rig description (DIRG-PoliTo)

The experimental setup assembled in the lab of DIRG-PoliTo is equipped with an electro-spindle, its power supply, three bearings and their supports, a load applying mechanism and a load cell. Two accelerometers are mounted on the structure, one on the support of the damaged bearing and the other on the support of the central bearing, devoted to the application of the external load. The acceleration signals were acquired for 10 seconds with sampling frequency of 51.2 kHz. A Rockwell tool has been utilized to create conical indentation on the inner ring or on one of the rollers. The size of the resultant localized faults is given by the diameter of the cones base (150, 250, 450 μm).

3.2 Case 1

Data used for this case is from IMS [6] and a description of the experimental activity can be found in [5]. In this case, the acceleration signal from a bearing with an inner race defect is studied. The raw time signal is depicted in Figure 2a in which impulsive noise with relatively large amplitude can be detected.

The outcome of Fast Kurtogram is shown in Figure 2b and the SES of the node with the highest kurtosis is displayed in Figure 2d. The inner race ball pass frequency (BPFI) is not detectable and bearing is not diagnosable by using this method. The Autogram and the SES of the selected node can be seen in Figure 2c and e. The shaft frequency, BPFI and its sidebands spaced at shaft

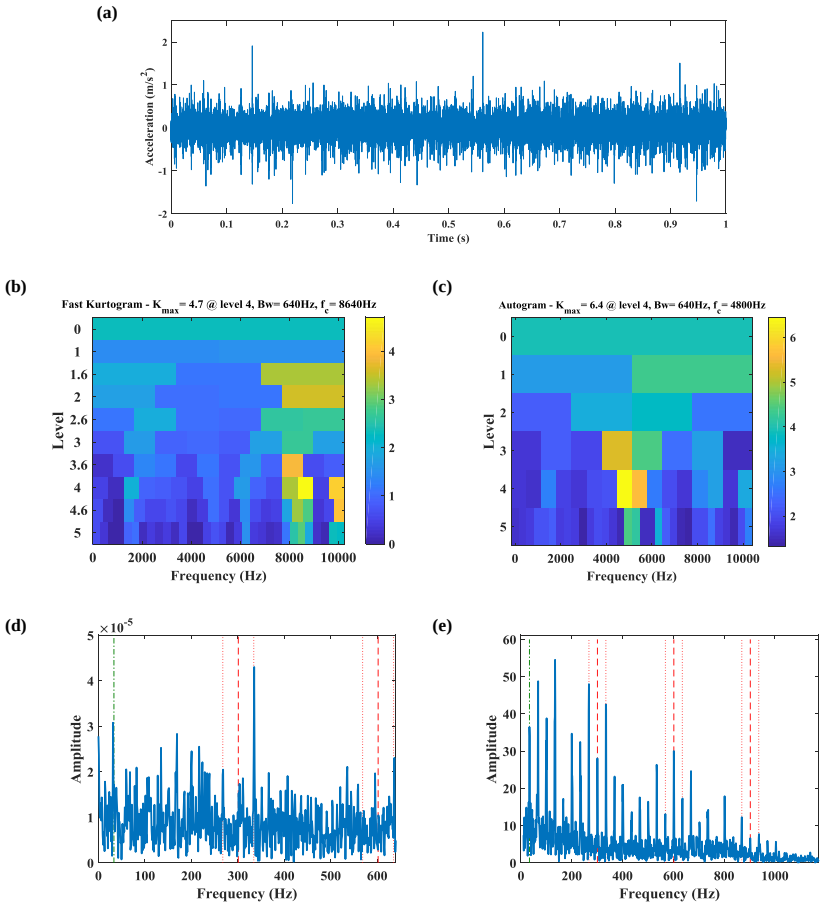

Fig. 2. Case 1, IMS data (first data set, channel 5 of data file 2003.11.25.15.47.32) **(a)** Time domain signal **(b)** Fast Kurtogram **(c)** Autogram; squared envelope spectrum (SES) of the signal related to node with highest kurtosis in **(d)** Fast Kurtogram **(e)** Autogram

frequency can be spotted clearly which result in a successful diagnosis. It should be mentioned that Fast Kurtogram is generally powerful method to extract the defect signal from background gaussian noise but its vulnerability to impulsive noise, which in common in industrial application, deteriorates its performance.

3.3 Case 2

Data are from DIRG-PoliTo and a faulty rolling element (indentation 150 μm) is under analysis. The signal is acquired by the sensor mounted on the casing of the same bearing.

Fast Kurtogram is depicted in Figure 3a and the SES for the selected node in Figure 3c does not provide any useful diagnostic information. In contrast, Autogram (Figure 3b) effectively finds the proper band for demodulation and the SES of its selected node (Figure 3d) allows the identification of the typical patterns of rolling element damage (Ball Spin Frequency (BSF) and sidebands spaced at Fundamental Train Frequency (FTF)). This result can be attributed to the low Signal-to-Noise Ratio (SNR) which leads Fast Kurtogram to achieve a maximum value of kurtosis of just 0.3.

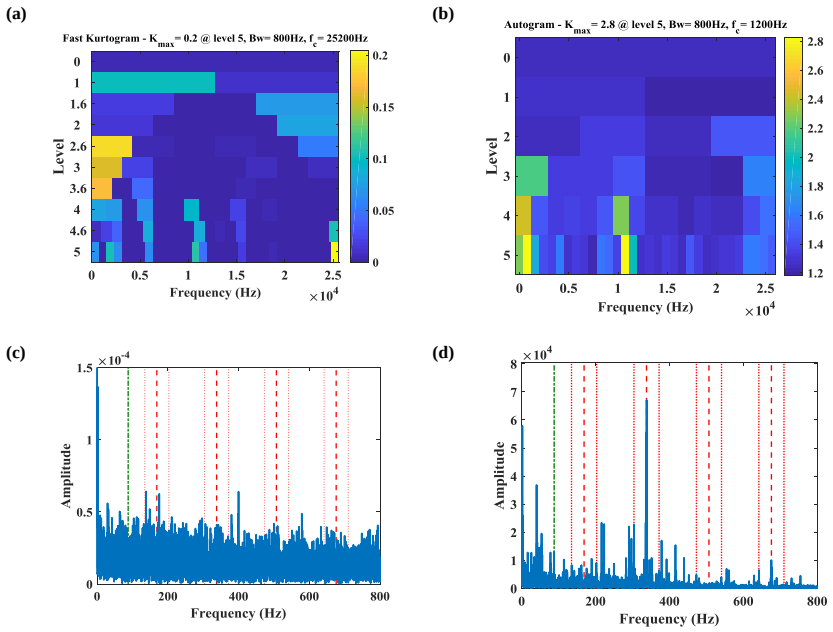

Fig. 3. Case 2, PoliTo data **(a)** Fast Kurtogram **(b)** Autogram; squared envelope spectrum (SES) of the signal related to node with highest kurtosis in **(c)** Fast Kurtogram **(d)** Autogram

3.4 Case 3

Also in this case data from DIRG-PoliTo are used. The rolling element defect is large (450 μm) but the signal is acquired by the sensor mounted on the central (undamaged) bearing casing. SES of the node selected by Autogram is depicted in Figure 4a (pink lines are at FTF). The Kurtogram -not shown here- provides similar results. Ball Spin Frequency (BSF) cannot be detected in this frequency band but the FTF (cage rotating frequency) dominates the SES.

In cases where the defect signal is weak, upper Autogram is preferable as it is more sensitive to repetitive transients even in presence of noise. In fact, it detects the frequency bands with valuable data more efficiently because the lower part, which mainly contains noise, is removed and the kurtosis values are increased. As a result, distinction between nodes with valuable information and other nodes is clearer. Therefore, the best option would be combination of CSES and upper Autogram. Nonetheless, it should be mentioned that upper Autogram may also be vulnerable to impulsive noise. The SES of the node selected by upper Autogram is plotted in Figure 4b. In comparison to the Autogram, the defect frequency is present in the SES of the node with the highest kurtosis.

The CSES and average CSES are shown in Figure 5 a and b. The CSES detects the BSF throughout level 1 to 5 but from the SES of the raw signal (level 0) this frequency cannot be found. For the sake of comparison, the result of Fast SC and full band Enhanced Envelope Spectrum (EES) [2] are depicted in Figure 6 a and b. The BSF is present in these two figures, although very weak.

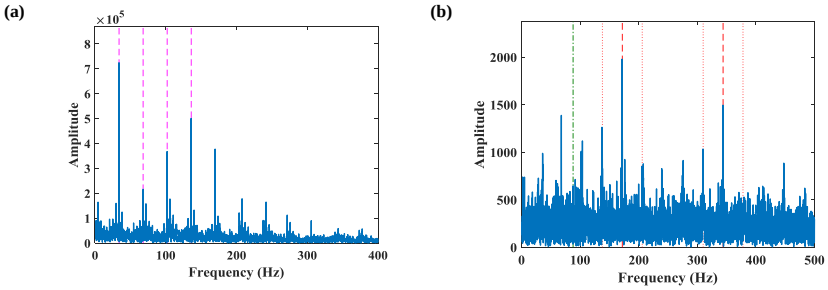

Fig. 4. Case 3, DIRG-PoliTo data. SES of the signal related to node with highest kurtosis in **(a)** Autogram (pink lines are at FTF) **(b)** upper Autogram

3.5 Case 4

The signal is again from DIRG-PoliTo. Data are recorded by the accelerometer on the damaged bearing, with a localized defect on the inner race (250 μm). Neither Autogram nor Fast Kurtogram are able to find the frequency band related to the defect signal. On the other hand, the combination of upper Autogram and CSES

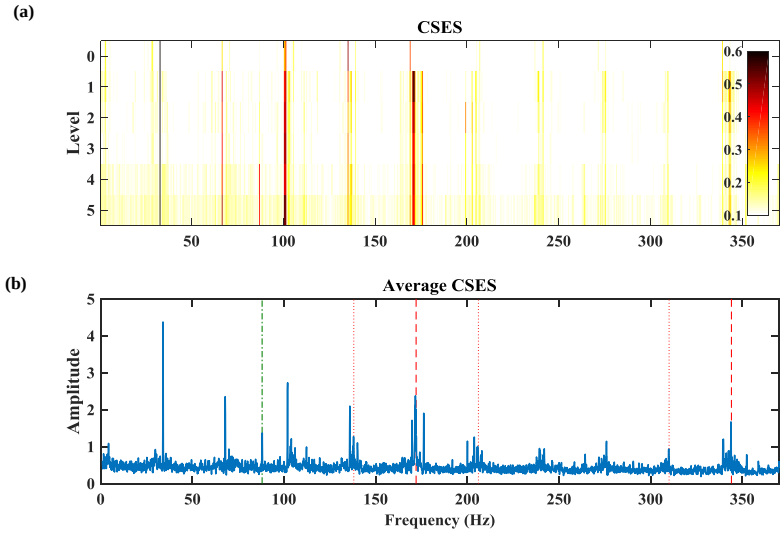

Fig. 5. Case 3, DIRG-PoliTo data **(a)** Combined Squared Envelope Spectrum (CSES) **(b)** average Combined Squared Envelope Spectrum (CSES) for all levels

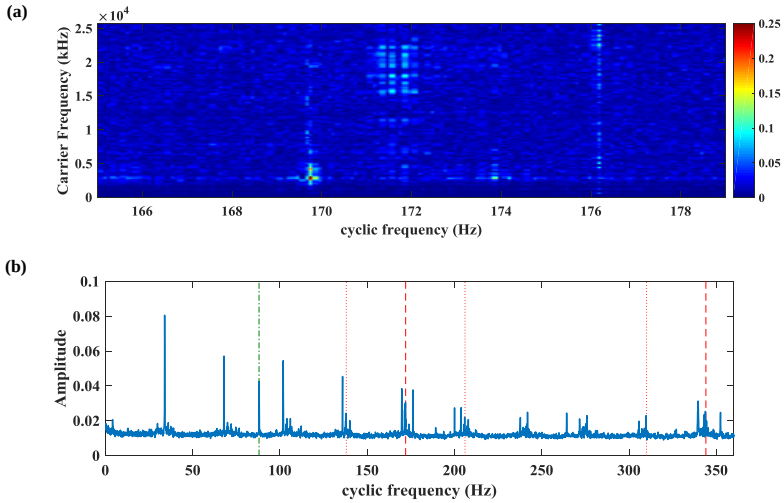

Fig. 6. Case 3, DIRG-PoliTo data **(a)** Fast Spectral Correlation **(b)** full band Enhanced Envelope Spectrum (EES)

(Figure 7 a and b) clearly demonstrate the presence of the fault throughout levels 1 to 4. Level 0 (raw signal) and 5 do not provide the defect signature and the shaft frequency dominates the SES.

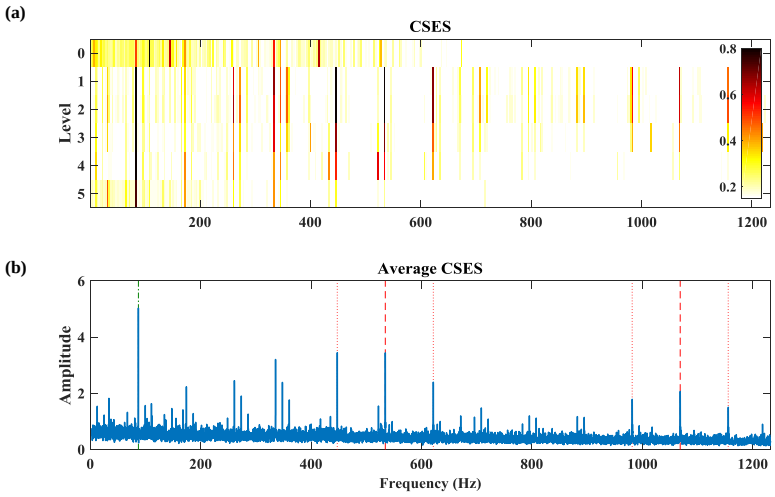

Fig. 7. Case 4, DIRG-PoliTo data **(a)** CSES **(b)** average CSES

The full band EES is shown in Figure 8 a. The presence of defect can be noticed in this figure although the BPFI is not the dominant frequency. The EES for the selected band [14 20.4] kHz is depicted in Figure 8b. In this case, the BPFI is clearly detectable and the spectrum is similar to CSES in Figure 7b. In general, EES for selected frequency bands where a specific cyclic frequency, such as a bearing defect frequency, is present, can provide better outcomes. The major disadvantage is that this frequency band should be found and set manually.

4 Conclusion

In this paper the performance of a recently proposed method, Autogram, has been investigated. Four different cases were studied from two different test rigs. The results of the first case show the better performance of the Autogram over Fast Kurtogram which is one of the mostly used method for diagnosis of rolling element bearings. In practice, when impulsive noise unrelated to a defect signal exists or in cases with relatively low Signal-to-Noise Ratio (SNR), Autogram has superior performance. In addition, the performance of upper Autogram and a novel indicator named Combined Squared Envelope Spectrum (CSES) was compared to Spectral Correlation (SC) which is a powerful tool to analyze cyclostationary signals and extracting hidden periodicities. Overall, CSES can provide

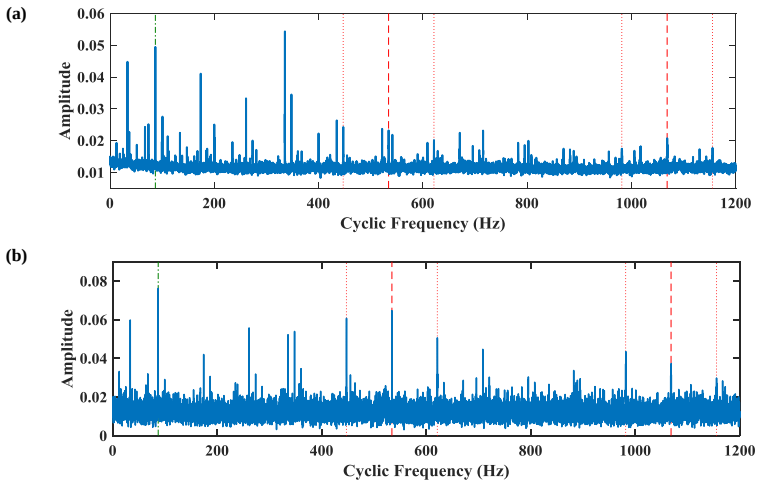

Fig. 8. Case 4, DIRG-PoliTo data **(a)** full band EES **(b)** EES for selected frequency band [14 20.4] kHz

comparable and in some cases even better results than full band Enhanced Envelope Spectrum (EES). On the other hand, EES for a selected frequency band generally offers notable results even for difficult cases but a manual selection of the correct frequency band for demodulation is compulsory.

References

1. Antoni, J.: Fast computation of the kurtogram for the detection of transient faults. Mechanical Systems and Signal Processing 21(1), 108–124 (2007)
2. Antoni, J., Xin, G., Hamzaoui, N.: Fast computation of the spectral correlation. Mechanical Systems and Signal Processing 92, 248–277 (2017)
3. Moshrefzadeh, A., Fasana, A.: The autogram: An effective approach for selecting the optimal demodulation band in rolling element bearings diagnosis. Mechanical Systems and Signal Processing 105, 294–318 (2018)
4. Antoni, J.: Cyclic spectral analysis in practice. Mechanical Systems and Signal Processing 21(2), 597–630 (2007)
5. Qiu, H., Lee, J., Lin, J., Yu, G.: Wavelet filter-based weak signature detection method and its application on rolling element bearing prognostics. Journal of sound and vibration 289(4-5), 1066–1090 (2006)
6. NASA Ames prognostics data repository, https://ti.arc.nasa.gov/tech/dash/groups/pcoe/prognostic-data-repository/